Quenching of Star Formation in Massive Clusters – Lynx W caught in the act

Inger Jørgensen[1], Kristin Chiboucas[1], Marcel Bergmann[1], Sune Toft[2], Ricardo Schiavon[3]
[1]Gemini Observatory USA; [2]DARK/NBI Copenhagen Denmark; [3]Liverpool John Moores University, UK

Perseus z=0.018 — Poster # 16 — Coma z=0.024

Abstract: We present results from our investigation of galaxy evolution in dense cluster environments up to redshift z=1.3 based on high S/N ground-based spectroscopy and HST imaging of bulge-dominated galaxies.

Quenching of star formation in Lynx W - Massive clusters from z=1.3 to the present:

Figures 2-6 show our results leading to the conclusion that RXJ0848.6+4453/Lynx W (z=1.27) is in the process of quenching the star formation throughout the cluster. The data show no evidence of size evolution. The Fundamental Plane, ages and star formation for Lynx W and our data for three rich galaxy clusters at z=0.5-0.9 are consistent with z_{form}~2. The results are published in Jørgensen & Chiboucas (2013) and Jørgensen et al. (2014).

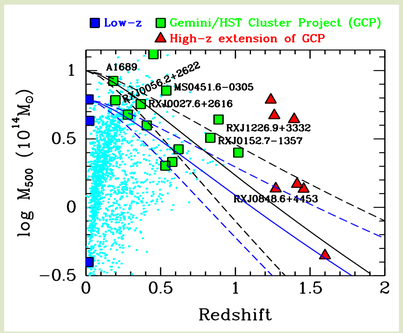

Fig 1: Cluster masses versus redshift for our cluster sample: *Since cluster masses grow over time, lower mass clusters at higher redshift, e.g. RXJ0848.6+4453/ Lynx W, are viable progenitors for higher mass clusters at lower redshift.* Large points – our full cluster sample with clusters covered in this poster labeled. Small blue points – X-ray cluster data (Piffaretti et al. 2011). Black and blue lines – sample models for evolution in cluster masses with redshifts based on van den Bosch (2002).

Ages, Metallicity, and Abundance Ratios from z=0.9 to the present:

Figures 8-10 show our analysis of spectroscopic data for six massive clusters at z=0.2-0.9. Results for the z>0.5 clusters are included in Jørgensen & Chiboucas (2013) while the results for the z=0.2-0.4 clusters are being prepared for publication. Ages are in general agreement with the last major star formation episode taking place at z~2, followed by quenching of the star formation as seen in Lynx W. Two of the clusters show differences in metallicity or [α/Fe] relative to the bulk of the clusters.

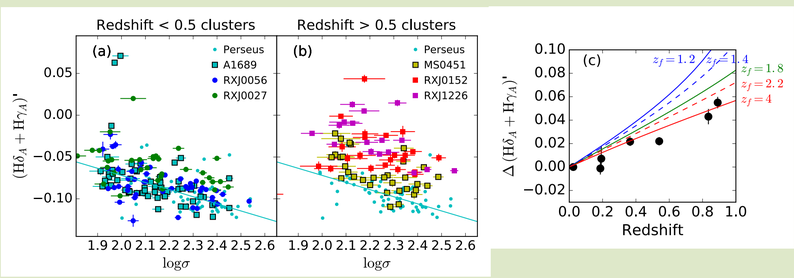

Fig 8: Balmer line strengths versus the velocity dispersions of the galaxies. The index-velocity dispersion relation for z~0 is shown for reference on panels (a)-(b). Panel (c) shows the median zero point differences relative to the z~0 relation. Passive evolution models based on Thomas et al. (2011) are shown for z_{form}=1.2 to 4.0. *The changes of the Balmer lines Hδ and Hγ with redshift are consistent with passive evolution with z_{form}~4. This assumes that all the clusters have the same mean metallicity and the same mean abundance ratios.*

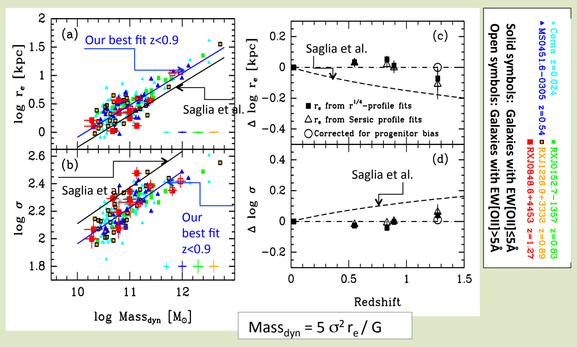

Fig 2: Size and velocity dispersion evolution for bulge-dominated galaxies: *The z<0.9 galaxies show no significant evolution of size or velocity dispersion with redshift. At z=1.27 sizes are smaller and velocity dispersion larger than at lower redshift at the 1-1.5-sigma level. However, once progenitor bias is taken into account, galaxies in Lynx W at z=1.27 also show no evolution in sizes or velocity dispersions (circles on panels [c] and [d]).* Progenitor bias correction was done by excluding z~0 galaxies with strong Hβ absorption (ages <8.3Gyr). Comparing to the evolution found by Saglia et al. (2010) [dashed lines on panels (c) and (d)] our results (at z=0.86) represent a 5-sigma difference for r_e and an 8-sigma difference for the velocity dispersion.

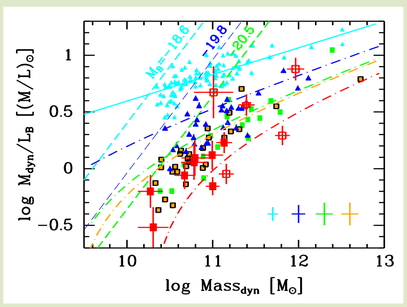

Fig 3: The Fundamental Plane as M/L versus Mass: *The z=0.5-1.3 cluster data are in agreement with a mass dependent formation redshift z_{form} to be understood as the epoch of the last major star formation.* Dashed-dotted blue, green, orange, red – passive evolution models based on formation redshifts z_{form} dependent on galaxy masses (or velocity dispersions) from Thomas et al. (2005), color coded to match the clusters that they model. For the z=0.5-0.9 clusters we find z_{form}=1.24±0.1 at $10^{10.6}$ $M_\odot$ and 1.95±0.25 at $10^{11.4}$ $M_\odot$. For Lynx W we find a slightly higher formation redshift at a given mass, z_{form}=1.95±0.2 at 10^{11} $M_\odot$. The result for the high mass galaxies is in agreement with results from van Dokkum & van der Marel (2007).

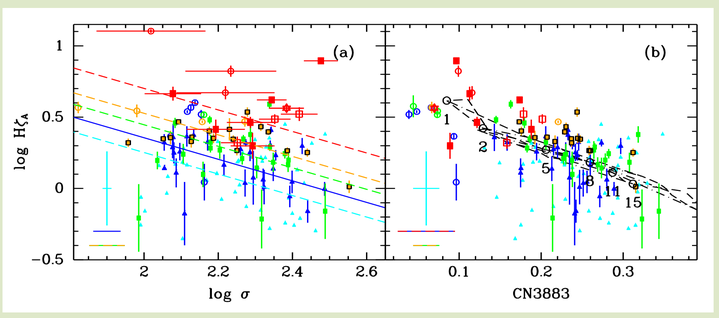

Fig 4: Absorption line indices. *The Hζ strength for bulge-dominated galaxies varies with redshift in agreement with the z_{form} from M/L versus Mass.* Lines on panel [a] show the best fit relation to the MS0451.6-0305 sample (solid) and relations offsets relative to that (dashed). Single stellar population (SSP) models from Maraston & Strömbäck (2011) on panel [b] are labeled with ages in Gyr at points corresponding to solar metallicity. Disk-dominated galaxies are shown as circles on both panels.

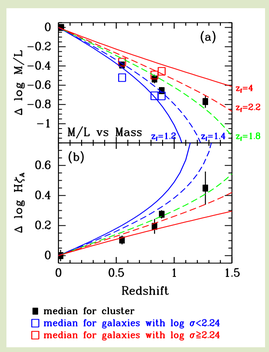

Fig 5: Zero point offsets of scaling relations relative to the z=0 sample: *The offsets for the M/L-Mass and Hζ-σ relations support that the last major star formation episode took place at z_{form}≈2.* Solid and dashed lines - passive evolution models for z_{form} as labeled based on SSP models from Maraston & Strömbäck (2011).

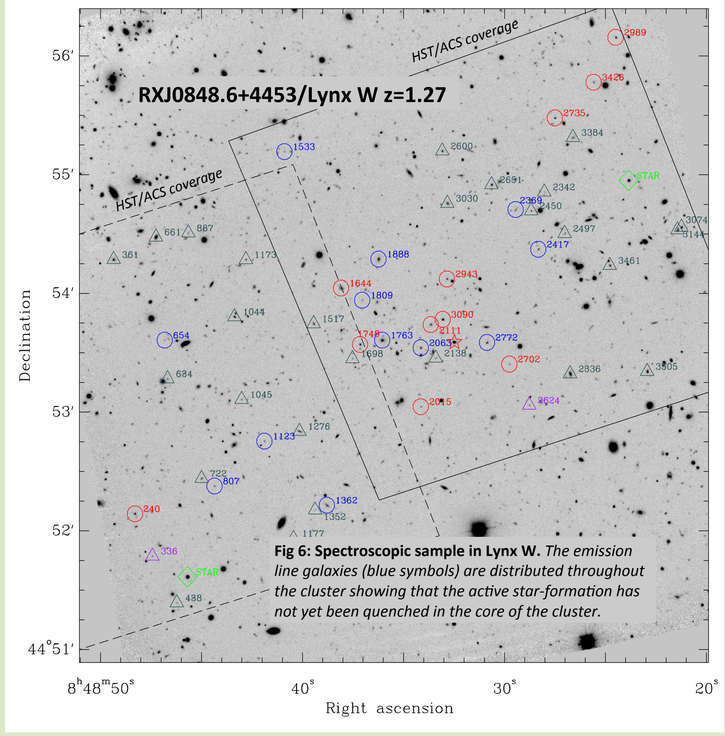

Fig 6: Spectroscopic sample in Lynx W. *The emission line galaxies (blue symbols) are distributed throughout the cluster showing that the active star-formation has not yet been quenched in the core of the cluster.*

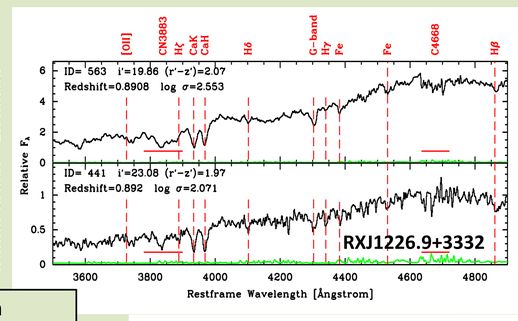

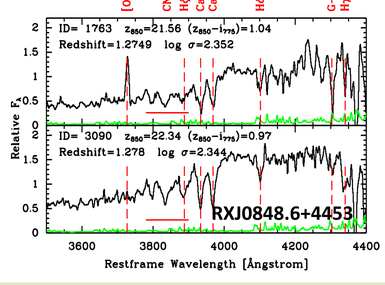

Fig 7: Sample spectra of RXJ1226.9+3332 and RXJ0848.6+4453 galaxies. Black – spectra in the rest frame. Green – 2x noise.

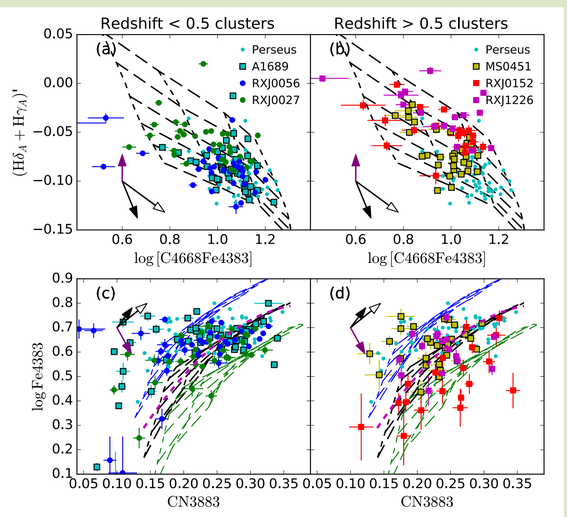

Fig 9: Absorption line indices versus each other. The grids show single stellar population (SSP) models from Thomas et al. (2011); blue, black and green are [α/Fe]=0, 0.3, and 0.5, respectively. The arrows indicate the direction of changes in age (solid black), [M/H] (open), [α/Fe] (solid purple). The index [C4668Fe4383] is constructed to have minimal dependency on [α/Fe], and only the [α/Fe]=0.3 model grid is shown on these panels. *The changes of the Balmer lines Hδ and Hγ with redshift are consistent with passive evolution. However, the index-index panels indicate variations in both [M/H] and [α/Fe], which are inconsistent with passive evolution.*

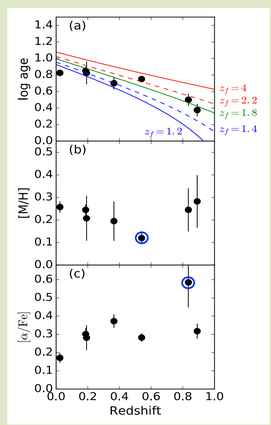

Fig 10: Mean ages, metallicity [M/H] and abundance ratios [α/Fe] for the clusters as a function of redshift. Solid and dashed lines on panel (a) show passive evolution models for formation redshift z_{form} as labeled based on Thomas et al. (2011). *Derived ages based are in general agreement with passive evolution with z_{form}~2. However, the cluster-to-cluster variations seen in [M/H] and [α/Fe] (circled in blue) are inconsistent with this simple model. The lower z_{form} than found from Hδ and Hγ alone [Fig 8] may be due to these differences not being taken into account for that determination.*

Conclusions:

- For bulge-dominated galaxies at a given mass we find no significant size or velocity dispersion evolution with redshift between z=1.27 and the present. This is in disagreement with results for less dense environments (Saglia et al. 2010) and indicates a larger difference in the evolution of field and cluster galaxies than found by Delaye et al. (2014) [Fig 2].
- The Fundamental Plane (M/L vs. Mass) for z=0.5-0.9 is consistent with passive evolution and mass dependent formation redshifts: z_{form}=1.24±0.1 and 1.95±0.25 for low and high mass galaxies, respectively. For Lynx W (z=1.27) z_{form}=1.95±0.2 at 10^{11} $M_\odot$ [Fig 3, 5a].
- The bulge-dominated galaxies in Lynx W have strong Hζ absorption [Fig 4] and many have [OII] emission. The emission line galaxies are distributed throughout the cluster [Fig 6]. The strong Hζ absorption is in agreement with z_{form}≈2 [Fig 4, 5b].
- The M/L ratios, Hζ absorption and [OII] emission of the Lynx W bulge-dominated galaxies are consistent with a major cluster-wide star formation episode 1-2 Gyr prior to the epoch of the cluster redshift combined with low level on-going star formation indicating that the star formation has not yet been fully quenched in the center of this cluster [Fig 6].
- Ages of bulge-dominated galaxies in z=0.2-0.9 clusters are in general agreement with the last major star formation taking place at z_{form}~2, followed by rapid quenching as seen in Lynx W [Fig 8-10].

References:
Delaye et al. 2014, MNRAS, 441, 203
Jørgensen & Chiboucas, 2013, AJ, 145, 77
Jørgensen et al. 2014, AJ, 148, 117
Maraston & Strömbäck, 2011, MNRAS, 418, 2785
Piffaretti et al. 2011, A&A, 534, A109
Saglia et al. 2010, A&A, 524, A6
Thomas et al. 2005, ApJ, 621, 673
Thomas et al. 2011, MNRAS, 412, 2183
van Dokkum & van der Marel, 2007, ApJ, 655, 30
van den Bosch, 2002, MNRAS, 331, 98

Acknowledgements: Based on observations obtained at the Gemini Observatory, which is operated by AURA under a cooperative agreement with the NSF on behalf of the Gemini partnership. Based on observations made with the NASA/ESA Hubble Space Telescope, obtained from the data archive at the Space Telescope Science Institute. IJ acknowledges support from grant HST-AR-13255.01 from STScI.